

Multi-Frequency Monitoring of Three Gamma-Ray Quasars

Svetlana Jorstad^{*†}, Alan Marscher^{*}, Ian McHardy^{**}, Kristopher Makrides^{*}, Daniel Salem^{*}, Thomas Balonek[‡], Jeyhan Kartaltepe[‡], Margo Aller[§], Valerij Larionov[†], Natalia Efimova[†], Claudia Raiteri[¶], Massimo Villata[¶], Omar Kurtanidze^{||}, Martin Gaskell^{††} and Marc Türler^{‡‡}

**Inst. for Astrophysical Research, Boston Univ., 725 Commonwealth Ave., Boston, MA 02215*

†Sobolev Astronomical Inst., St. Petersburg State Univ., Universitetskij pr. 28, St. Petersburg, 198504 Russia

***Dept. of Physics, Univ. of Southampton, Southampton SO17 1BJ, UK*

‡Dept. of Physics and Astronomy, Colgate Univ., 13 Oak Dr., Hamilton, NY 13346

§Astronomy Dept., Univ. of Michigan, 830 Dennison, 501 East University St., Ann Arbor, Michigan 48109

¶Osservatorio Astronomico di Torino, Via Osservatorio, 20, 10025 Pino Torinese, Italy

||Abastumani Obs., 383762, Abastumani, Georgia

††Dept. of Physics and Astronomy, Univ. of Nebraska, Lincoln, NE 68588

‡‡Geneva Obs., ch. des Maillettes 51, CH-1290 Sauverny, Switzerland

Abstract. We have performed two campaigns of intensive monitoring of the blazars 3C 273, 3C 279, and PKS 1510–089 in the X-ray, optical, near-IR, and radio regions in March and April 2002. The quasar 3C 279 reveals significant interday variability at all wavelengths. The quasar 3C 273 shows smooth variations in the X-ray and near-IR regions on time scales of 2-3 days. For both quasars the results indicate close connection between X-ray and near-IR emission with a delay of X-rays from 0 to 3 days. The quasar PKS 1510-089 was in a low emission state at all frequencies during the campaigns.

INTRODUCTION

Blazars form the most energetic subclass of active galactic nuclei (AGN) characterized by violent variability on time scales from hours to years across the electromagnetic spectrum [9, 14, 13]. It is commonly thought that in the radio, infrared (IR) and optical regions the variable emission of blazars originates in relativistic jets and is synchrotron in nature, while the origin of the high energy emission is less clear. There are observational and numerically simulated results [7, 1, 6] that suggest that the X and γ -rays are produced in the relativistic jets as well. The most popular models for the high energy production involve inverse-Compton scattering of low energy photons by the relativistic electrons. This implies the existence of correlated behavior between low and high energy emission. However, the origin of the seed photons is uncertain. They might be synchrotron photons from the jet (SSC model) or external to the jet (EC process, [12]). The models can be distinguished by measuring time lags between the seed and Compton-scattered variations [8]. Therefore, simultaneous multifrequency campaigns as in [5, 2] are crucially important for establishing a detailed model of blazar activity and for constraining the physics of relativistic jets.

OBSERVATIONS

The X-ray observations of the quasars are part of a long-term monitoring program of blazars performed with the Rossi X-ray Timing Explorer (RXTE) starting in Cycle 1 and continuing to at least 2005 (see Marscher et al., these proceedings). The intensive X-ray observations (3-5 points per day) of 3C 273 and 3C 279 were carried out in Cycle 7 from April 8 to April 17 2002 and of the quasar PKS 1510–089 from May 14 to May 20 2002. The observations were made with the large-area Proportional Counter Array (PCA) [3]. The PCA data were edited and calibrated using the FTOOLS software, version 5.2. Single power-law spectral model fits were obtained with XSPEC, version 11.2. The fits included photoelectric absorption based on the column density of neutral hydrogen in our Galaxy. The background count rate was calculated using the RXTE *L7* faint source background model. This procedure provided fluxes and spectral indices over the energy range of 2.4-20 keV (2.4-10 keV for 3C 279).

The optical and IR observations were performed at different telescopes around the world, listed in Table 1. Column 4 of the table gives the symbol used to plot the data in Figures 1-3. We used comparison stars 4

and 6 for 3C 273, 2 and 9 for 3C 279 and 1, 7, and 9 for PKS 1510–089 from [4] to obtain the standard magnitudes in the optical region. Comparison star 9 also was used to determine the standard J and K magnitudes for PKS 1510–089. The IR observations of 3C 273 and 3C 279 were performed only at the Perkins telescope at Lowell observatory where the IR camera has a field of view $66'' \times 66''$ which does not include comparison stars for these quasars. In this case, the observational strategy involved switching between J, H measurements of the quasars and comparison star FS132 ($K = 11.836 \pm 0.004$) from the UKIRT list of standard stars, located $\sim 2^\circ$ and $\sim 5^\circ$ from 3C 273 and 3C 279, respectively. The data were checked for bad and unreliable points by comparison of measurements for each night separately and corrected for the offsets between different datasets. The absolute calibration by [10] was applied to transform magnitudes to fluxes.

Simultaneous radio observations were performed at 4.5, 8, and 14.5 GHz at the 26-m telescope at the University of Michigan Radio Astronomy Observatory.

RESULTS

The light curves are shown in Figures 1-3. During the campaign the quasar 3C 273 gradually decreased in X-ray flux by $\sim 25\%$ (the uncertainty of an individual observation is $\sim 3\%$) and faded at IR-wavelengths by $\sim 18\%$ (the uncertainty of an individual observation is $\sim 5\%$). The quasar 3C 279 underwent a moderate flare on a time scale of about 3 days in the optical and IR regions, with more random interday variations in X-rays with amplitude $\sim 10\%$. The quasar PKS 1510–089 was in a faint phase. The interday variations of PKS 1510–089 at all frequencies from X-rays to radio did not exceed uncertainties of individual measurements. Figure 4 presents the spectral energy distribution (SED) of the quasar at this low state of emission. The dotted line approximates the SED by the power law $S_\nu \propto \nu^{-\alpha}$, with $\alpha = 0.78 \pm 0.02$. This fits the SED from the radio to optical regions very well while the X-ray emission exceeds the extrapolated synchrotron X-ray emission significantly.

CROSS-CORRELATION ANALYSIS

In order to determine the level of correlation of the light curves at different frequencies, we binned the data for 3C 273 and 3C 279 in time intervals of 0.2 days at all wavelengths and interpolated linearly between observed points. The interpolated light curves are shown in Figures 1,2 by dotted lines. These evenly binned light curves were used to perform the standard cross-correlation (CC)

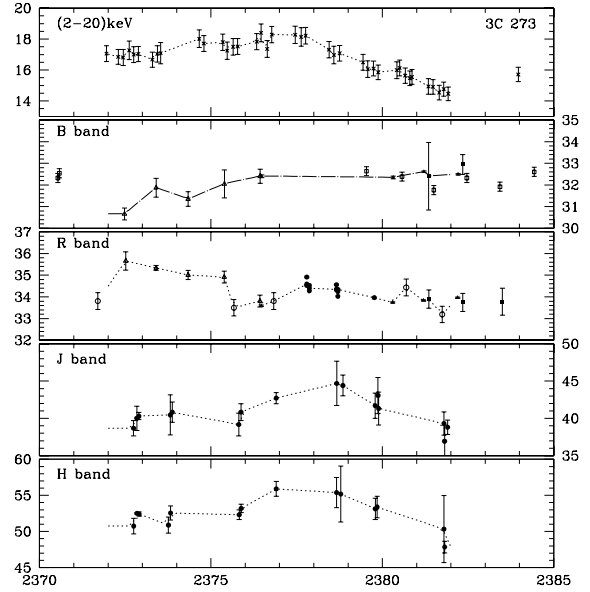


FIGURE 1. Light curves of the quasar 3C 273 during the campaign. The X-ray flux is in units $10^{-11} \text{erg cm}^{-2} \text{s}^{-1}$, the optical and IR flux is in mJy.

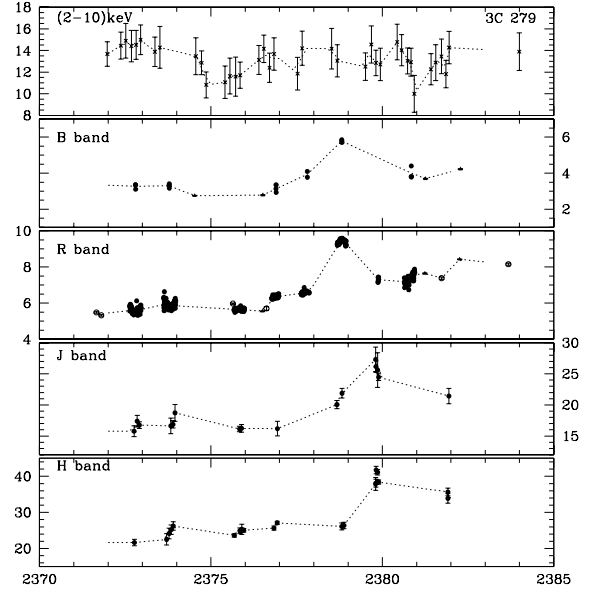


FIGURE 2. Light curves of the quasar 3C 279 during the campaign. The X-ray flux is in units $10^{-12} \text{erg cm}^{-2} \text{s}^{-1}$, the optical and IR flux is in mJy.

analysis. Figures 5 and 6 present the cross-correlation of the light curves shown in Figures 1 and 2, respectively, with the following designations: XR (solid curve) - CC-function between the X-ray and R-band light curves, XH (dotted) - CC-function between the X-ray and H-band light curves, BR (short-dashed) - CC-function between

TABLE 1. List of participating observatory by longitude

Observatory	Tel. size (cm)	Filter	Symbol
Abastumani, Georgia	70	B,V,R,I	triangle
Crimean, Ukraine	70	B,V,R,I	filled triangle
Campo Imperatore, Italy	110	J, H	diamond
Torino, Italy	105	B,V,R,I	filled square
La Silla, Chile		U,B,V	square
Foggy Bottom, USA	30	R	circle
Univ. of Nebraska, USA	40	V	
Lowell, USA	180	J,H,K	filled circle
Lowell, USA	90	U,B,V,R,I	filled circle

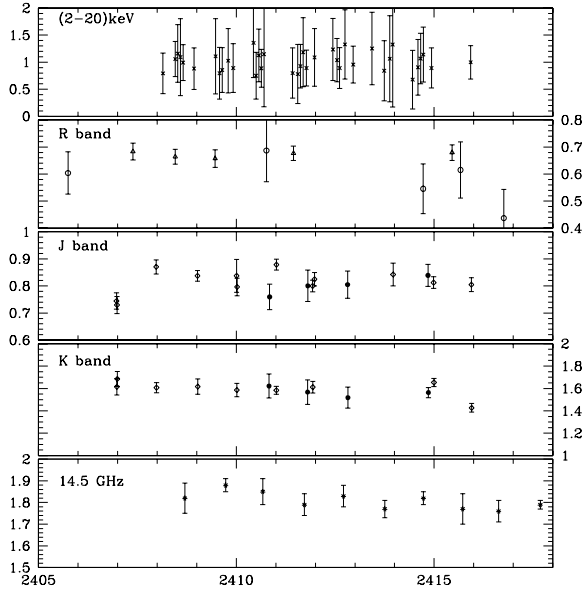


FIGURE 3. Light curves of the quasar PKS 1510–089 during the campaign. The X-ray flux is in units $10^{-11} \text{erg cm}^{-2} \text{s}^{-1}$, the optical and IR flux is in mJy, the radio flux is in Jy.

the B and R-band light curves, RH (long-dashed) - CC-function between the R and H-band light curves, and JH (dash-dotted) - CC-function between the J and H-band light curves.

3C 273. The formal cross-correlation analysis indicates (Fig. 5) that there is a strong correlation between the infrared emission in J and H bands, although the behavior in the blue (*B*-band) and red (*R*-band) parts of the optical region is strongly anticorrelated (on the other hand, the fractional variation in both *R* and *B* is very small). There is a moderate correlation between the *R*-band and infrared light curves with a delay of the former by 4.8 ± 1.2 days. This implies that the variable part of the red optical emission comes from the same source as the IR emission (jet?), while a different source (accre-

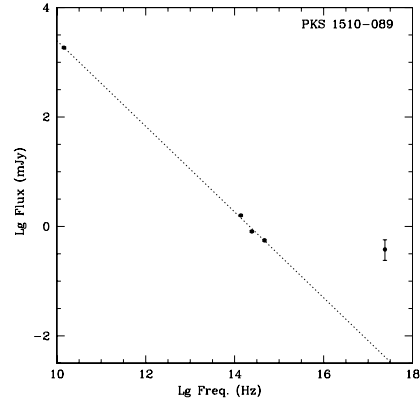


FIGURE 4. SED of the quasar PKS 1510–089

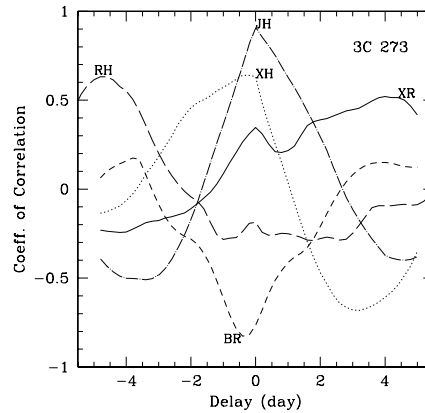


FIGURE 5. Cross-correlation of the light curves for 3C 273. Negative delay corresponds to the variations in the first band leading those in the second.

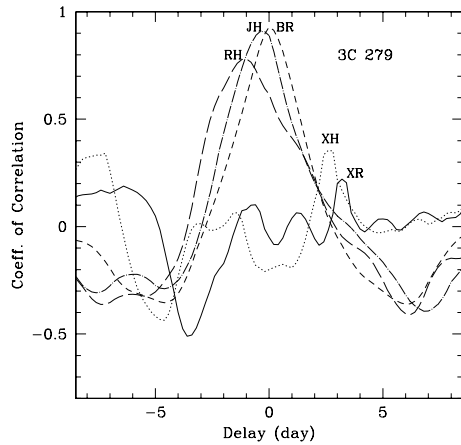


FIGURE 6. Cross-correlation of the light curves for 3C 279. Negative delay corresponds to the variations in the first band leading those in the second.

tion disk?) is responsible for the variations of the blue optical emission. There is a possible connection between the X-rays and R-band with an uncertain delay of the X-ray emission from 0 to 4 days. The CC-function between X-ray and H-band light curves is very similar to the CC-function obtained by [11] between the X-ray and K-band light curves during the campaign in 1997. They found that the highest correlation coefficient (~ 0.8) corresponds to a delay of the X-rays by 0.75 ± 0.25 days, although a lag of the IR by up to 5 days is possible. In our case the highest correlation coefficient (~ 0.6) is observed between X-ray and H-band emission without a delay, although a lag of the IR by up to 2 days is possible.

3C 279. In the case of the quasar 3C 279 (Fig. 6) there is a strong correlation between the optical B and R bands and between the infrared *J* and *H* bands. The *H*-band light curve has a lag of ~ 0.2 days relative to *J* band that might be caused by the size of the binning. A good correlation is observed between the optical and IR regions with the R-band emission leading by ~ 1 day. A connection between the X-ray and IR emission is possible with *H*-band leading X-ray by ~ 2.5 days or X-ray preceding IR emission by ~ 7.5 days. However, the former coefficient of correlation is based on fewer points (14) than the peak corresponding to *H*-band leading (38).

DISCUSSION

The cross-correlation analysis indicates that there is positional stratification of regions responsible for the variable emission at different frequencies: the optical region

is closer to the site of particle acceleration (central engine or shock front) and the IR region is located farther from the accelerator by 1 – 4 light travel days. The optical and infrared emission are produced via the synchrotron mechanism while the observed X-ray emission is significantly higher than that of the extrapolated synchrotron spectrum and shows a delay relative to the optical-IR synchrotron photons by 0 – 3 days. This implies that the same relativistic electrons that produce IR-emission (the highest coefficients of correlation are obtained between X-ray and IR light curves) participate in the production of the variable X-rays. Therefore, the variable X-ray emission originates in relativistic jets in the same region as the IR emission. The derived lags are consistent with the most popular model for the X-ray production that involves scattering of the low energy photons by relativistic electrons where the seed photons are the synchrotron (IR) photons from the jet (SSC-model). The X-ray variations are delayed relative to IR flares by the light travel time required for the low energy photons to cross the emission region to be scattering (see Sokolov & Marscher, these proceedings).

ACKNOWLEDGMENTS

The work was supported in part by the National Science Foundation under grant AST-0098579 and by NASA under grants NAG5-11811 and NAG5-13074. We thank students Peter R. Forshay (Haverford College) and Joseph G. Martin (Colgate University) for participating in optical observations of PKS 1510–089 at Foggy Bottom Observatory.

REFERENCES

1. Bloom, D.C. et al. 1999, ApJS, 122, 1
2. Böttcher, M. et al. 2003, ApJ, 596, 847
3. Bradt, H.V.D., Rothschild, R.E., Swank, J.H. 1993, A&AS, 97, 355
4. González-Pérez, J.N., Kidger M.R. & Martín-Luis, F. 2001, AJ, 122, 2055
5. Hartman, R.C. et al. 2001, ApJ, 553, 683
6. Jorstad, S.G., et al. 2001, ApJ, 556, 738
7. Lister, M.L. & Marscher, A.P. 1997, ApJ, 476, 572
8. Marscher, A.P. 1996, ASP Conf. Ser., 110, 248
9. Mattox, J.R., et al. 1997, ApJ, 476, 692
10. Mead, A.R.C. et al. 1990, A&AS, 83, 183
11. McHardy, I. et al. 1999, MNRAS, 310, 571
12. Sikora M., Begelman M.C., & Rees M.J. 1994, ApJ, 421, 153.
13. Terästranta H. et al. 1998, A&AS, 132, 305
14. Villata, M., et al. 2002, A&A, 390, 407